Observations and snow model simulations of winter energy balance terms within and between different coniferous forests in southern boreal Finland

Sirpa Rasmus, David Gustafsson, Robin Lundell and Timo Saarinen

ABSTRACT

Variation of canopy properties between different forest types is seldom taken into account in hydrological and climate models, and consideration of variation inside a forest is normally omitted. In this work, three data sets on near surface energy balance terms (incoming shortwave and longwave radiation; air and snow–soil interface temperatures) were collected in the southern boreal coniferous zone in Finland during three winters below different types of forest canopies. The aim was to evaluate the ability of a snow mass and energy balance model with a canopy module to reproduce the observed differences in below-canopy incoming radiations and snow–soil interface temperature. Clear differences were seen between pine and spruce forest sites (higher snow–soil interface temperatures and incoming shortwave fluxes, and lower incoming longwave fluxes at the pine site). Differences were also observed between the sparse and dense pine canopy locations. Canopy parameter values had a great effect on the quality of the model simulations. The combination of optically obtained leaf area index (LAI) values with a needle clumping correction and either optical or empirical sky view fraction (SVF) values as a canopy parameterization gave better correspondence to observations than the use of uncorrected effective LAI and any SVF.

Key words | canopy, coniferous forests, radiation, snow, snow modeling, snow–soil interface temperature

Sirpa Rasmus (corresponding author)
Department of Biological and Environmental Sciences,
University of Jyväskylä,
PO Box 35, (Survontie 9),
40014 Jyväskylä,
Finland
E-mail: *sirpa.rasmus@jyu.fi*

David Gustafsson
Department of Land and Water Resources Engineering,
Royal Institute of Technology, KTH,
Valhallavägen 79,
100 44 Stockholm,
Sweden

Sirpa Rasmus
Robin Lundell
Timo Saarinen
Plant Ecophysiology and Climate Change Group (PECC), Department of Biosciences,
University of Helsinki,
PO Box 65, (Viikinkaari 1),
00014 Helsinki,
Finland

INTRODUCTION

The boreal environment is governed by forests and by winter. The coniferous forest canopy has been shown to affect spatial patterns of snow depth and snow quality (e.g. Lundberg & Koivusalo 2003; Stähli & Gustafsson 2006; Veatch *et al.* 2009). Local differences in the canopy interception of snow lead to significant small-scale variation in the mass balance of boreal forest snow cover (Hardy & Albert 1995; Hedström & Pomeroy 1998; Link & Marks 1999).

The canopy is the governing factor in the snow surface energy exchange in boreal coniferous forests (Davis *et al.* 1997). Energy transfer to and from the snow include radiation, sensible and latent heat flux, soil heat flux, and heat flux by mass advection. Large spatial variability is seen both in incoming shortwave and incoming longwave radiation fluxes below coniferous forest canopies. The temporal persistence of the spatial distribution of the fluxes depends on the canopy structure and is different for longwave and shortwave fluxes (Essery *et al.* 2008).

In most of the cases, radiation is the primary source of energy for the snow cover below the forest canopy (Pomeroy & Dion 1996; Link & Marks 1999; Hardy *et al.* 2004). Observations at alpine sites show that radiation dominates the snow cover energy balance throughout the snow season, and radiation accounts for most of the energy available for snow melt (Marks & Dozier 1992; Davis *et al.* 1997). Incoming shortwave radiation is effectively attenuated by needles, branches and trunks; intercepted snow also affects the winter-time radiation levels in coniferous forests (Stähli

doi: 10.2166/nh.2015.177

et al. 2009). Spatial variability of the radiation components is important especially during snow melt (Pomeroy et al. 2008; Musselman et al. 2012a, b), most of the variability is due to variability in the direct beam component (Musselman et al. 2013). Litter on the snow surface or dark ground visible through the thinner snow cover often found near tree trunks lowers the albedo of the snow and thus may increase the amount of radiation absorbed (Melloh et al. 2001; Pomeroy et al. 2001).

There is also large spatial variability in the sub-canopy thermal regime and, consequently, in the longwave radiation reaching the snow surface (Rowlands et al. 2002). Shortwave radiation absorbed by the canopy is thermally radiated to the snow surface as longwave radiation. The highest shortwave radiation fluxes are observed in forest openings, but the highest longwave radiation values are observed close to warm, sunlit tree trunks (Essery et al. 2008).

The canopy also affects the snow evaporation in the forest by emitting longwave radiation during the night, keeping the snow surface relatively warm (Bernier & Swanson 1993). The canopy shelters the snow cover from turbulent heat exchanges of latent and sensible heat, which depend on wind speed and below-canopy temperature and humidity gradients (Harding & Pomeroy 1996; Storck et al. 1999). Canopy density (defined as fraction of overlying hemisphere occupied by canopy), and in heterogeneous forests also the size of the forest openings, affect the level of forest snow turbulent heat fluxes. Turbulent heat fluxes are relatively small, but they are important for the snow energy balance during mid-winter and toward the melting period (Koivusalo & Kokkonen 2002; Marks et al. 2008).

Snow is among the most important factors affecting the distribution of plants in alpine and arctic areas (Vestergren 1902; Billings & Bliss 1959). The spatial variability in the distribution of snow affected by the tree and canopy distribution has been shown to play a role in ground vegetation distribution even in a homogeneous Scandinavian pine forest (Rasmus et al. 2011). The effect of tree and canopy distribution on ground vegetation may be direct or indirect through the resulting variability in the snow cover (Økland et al. 1999; Rasmus et al. 2011). Under the snow, the intensity of photosynthetically active radiation (PAR) is low, as solar radiation is effectively absorbed by the snow (Curl et al. 1972; Gerland et al. 1999). Varying incoming shortwave radiation fluxes and snow depths within a forest lead to spatial variability in snow–soil interface temperature and in PAR, both above and below the snow, at the dwarf shrub level.

Snow modeling can be an efficient tool in hydrological and ecological applications. The Swiss SNOWPACK model (Bartelt & Lehning 2002; Lehning et al. 2002a, b) is an established and widely used model of snow mass and energy balance. It is one of the few existing snow structure models and can estimate with good temporal resolution the layered structure within the snow cover and the physical properties of the layers (grain size, form and bonding, snow temperature, density and hardness, volumetric fractions of ice, liquid water and air). A canopy sub-model recently included in the model enables estimating the forest snow properties. The use of the SNOWPACK in the forested areas is nevertheless limited because the canopy module has not been extensively tested.

The first aim of this study is to compare the wintertime ranges in incoming shortwave and longwave radiation and temperature regimes between two different types of southern boreal coniferous forest and within a single forest stand. The second aim is to use these observations to validate the ability of the model SNOWPACK to simulate the energy balance terms and temperature regimes of the snow below these different canopies. The effect of the choice of the canopy parameters on simulation quality is also addressed as part of the validation.

MATERIAL AND METHODS

Study location

Two sites with fairly flat topography in a pine and a spruce forest were chosen for the work. The study sites are located close to each other in Evo, southern Finland (61° 11′ N; 25° 5′ E, 130 m above sea level) with a mean annual temperature of 3.9 °C and mean annual precipitation of 630 mm. Locations for the radiation and temperature measurements within the forests were carefully chosen to ensure the representativeness of the observations when only a limited amount of observational devices – with fixed locations – could be used. Detailed mapping of the pine site was performed, including location of all trees taller than 0.5 m,

mean diameter at breast height and mean tree height of the trees taller than 2 m, and basal tree area of the site. The horizontal canopy dimensions of trees taller than 20 m were mapped with a modified Cajanus tube by locating the edge points of the canopy in eight different directions for each tree (Rautiainen *et al.* 2005). Based on these measurements, indices of tree influence on different points on the forest floor were calculated. The one-sided leaf area index (LAI), and corresponding canopy openness (or sky view fraction (SVF)) of the site were observed at a 1 m resolution using a Licor LAI-2000 Plant Canopy Analyzer along a 40-point transect at the mid-line of the site. Combining the information gained from mapping and LAI/SVF observations, locations representing sparse pine canopy (LAI 1.58 and SVF 0.33) and dense pine canopy (LAI 1.93 and SVF 0.19) were selected. The measurement location below the spruce canopy was based on the LAI and SVF transect observations (LAI 3.80 and SVF 0.15), representing spruce canopy with an average coverage. Both sites were estimated to have a mean canopy height of 14 m. A more detailed description of the spatial distribution of trees, canopy, ground vegetation and snow at the pine site can be found in Rasmus *et al.* (2011).

Observations on radiation components, temperature regimes and snow

Three data sets on incoming shortwave and longwave radiation and air and snow–soil interface temperatures were collected between October and April during winters 2007–2008 (in an open field and on the sparse location at the pine site), 2008–2009 (the sparse and dense locations at the pine site) and 2009–2010 (the sparse location at the pine site and the spruce site). Shortwave and longwave radiation was measured with Kipp&Zonen CM3 pyranometers and CGR3 pyrgeometers, respectively, that were mounted on a stand 1.5 m above ground (Figure 1). Air temperature 2 m above ground and snow–soil interface temperature below the dwarf shrub canopy were monitored using Pt-100 temperature probes (Campbell Scientific Inc., Logan, UT, USA). The temperature probes were protected from direct sunlight by a cylindrical radiation shield (height 20 cm, diameter 6 cm) made of white PVC plastic. All data were collected using a CR1000 Campbell Scientific datalogger logging every 10 min. The data were analyzed at three time resolutions: 3 h, daily and monthly.

Figure 1 | Setup of the radiation and temperature observational station at the open field site in Evo, southern boreal Finland.

Snow depth was observed manually twice a month between January and April (as a mean of a 40-point transect along the mid-line of the sites) at the pine and spruce sites during winter 2008/2009, and monthly at the sparse pine and the spruce locations during winter 2009/2010.

Snow model SNOWPACK and simulations

SNOWPACK is a one-dimensional model for snowpack structure, mass and energy balance, developed in the Swiss Federal Institute for Snow and Avalanche Research (SLF) for avalanche warning purposes. SNOWPACK is a predictive model that uses Lagrangian finite elements to solve for heat and mass transfer, stresses, and strains within the snow cover. The model is physically based: energy balance, mass balance, phase changes, water and water vapor movement are included, and the layer calculations are based on snow microstructure (crystal size and form, bond size, number of bonds per crystal). A complete

description of the model can be found in Bartelt & Lehning (2002) and Lehning *et al.* (2002a, b).

Recently a canopy sub-model has been added to the SNOWPACK model to simulate the impact of vegetation on the upper boundary conditions of the underlying snow cover. The canopy sub-model simulates in particular the transmission of shortwave and longwave radiation, turbulent heat exchange and precipitation interception and throughfall. The details of the canopy model can be found in previous publications (Lehning *et al.* 2006; Stähli *et al.* 2009; Musselman *et al.* 2012a, b; Rasmus *et al.* 2013) and only a summary is given here with special attention to the representation of radiation and interception processes and the influence of LAI and SVF. The canopy sub-model simulates the temperature and the storage of intercepted precipitation (frozen and unfrozen) in a single-leaf vegetation layer, characterized by three structural parameters: mean vegetation height, LAI and SVF. The canopy temperature is calculated by solving a canopy energy balance equation where the canopy net radiation is balanced by the sum of sensible and latent heat fluxes between the canopy and the atmosphere (the model version used in this study does not take into account any heat storage in the canopy). The basis for the radiation transmission model is the absorption of radiation as an exponential function of LAI following Beer's Law. The absorption coefficient for shortwave radiation includes the impact of solar elevation angle for direct beam path length through the canopy (Chen *et al.* 1997) and SVF (Gryning *et al.* 2001), multiple reflections between the canopy layer and the snow or soil surface below (Taconet *et al.* 1986), as well as the impact of intercepted snow on the canopy albedo as described in Stähli *et al.* (2009) and Musselman *et al.* (2012a, b). The transmission model for longwave radiation follows the same principles as for diffuse shortwave radiation, with constant SVF and radiation absorption as a function of LAI in the canopy covered fraction (1-SVF). The downward longwave radiation at the snow surface is a sum of radiation from the canopy as function of canopy temperature, and atmospheric radiation either transmitted through the canopy or directly through the gaps in the canopy corresponding to the fraction SVF. The parameter values for LAI and SVF are further used in the calculation of snow and rain interception and for the turbulent heat exchange between the snow surface and the atmosphere. The direct throughfall fraction is assumed equal to the SVF. The remaining precipitation is intercepted following the snow interception model suggested by Pomeroy *et al.* (1998) where the interception capacity is linearly related to LAI. The intercepted precipitation is evaporated as part of the canopy latent heat flux. Intercepted snow will be unloaded when air temperature is increased above 0 °C, when the snow interception capacity is assumed to be drastically reduced. The turbulent heat exchange is calculated using aerodynamic resistances between the atmosphere and the canopy air layer following the usual bulk-formulation based on displacement height and surface roughness length. Additional resistances are added for the fluxes from the canopy air layer to the canopy layer and the snow/soil layer, respectively, following the simplified two-layer model suggested by Blyth *et al.* (1999). The resistance between the snow/soil layer and the canopy layer is further increased as an exponential function of LAI (details available in Musselman *et al.* 2012a, b). SNOWPACK has been validated in several studies in varying climatic conditions (e.g. Lehning *et al.* 1998; Lundy *et al.* 2001; Rasmus *et al.* 2007); the canopy radiation transmission sub-model has been evaluated by Stähli *et al.* (2009) and Musselman *et al.* (2012a, b). In the present study, the snow cover part of the model was applied without calibration to local conditions in order to detect how well the radiation and temperature conditions could be reproduced by running the model with various canopy parameterizations.

The SNOWPACK model uses air temperature (°C), relative humidity (%), wind velocity (ms^{-1}) and direction (°), incoming shortwave and longwave radiation (Wm^{-2}) and precipitation (mm), either above the canopy or from an open area as meteorological input data. For the model runs in the present study, input data were obtained from the Finnish Meteorological Institute (FMI) station near the open field site, as the study data for the open site were limited to the winter 2007–2008. This observational data were nevertheless used for input data sensitivity tests. Synoptic meteorological observations with 3 h time resolution were used together with the FMI grid estimates of the incoming shortwave radiation of the site. Incoming longwave radiation was estimated using the difference between potential (theoretical value of incoming shortwave radiation not taking cloudiness

into account) and observed incoming shortwave radiation, air temperature and relative humidity of each 3 h time step (the method is described in Konzelmann *et al.* (1994)).

The model was run for the open, pine (sparse and dense) and spruce sites for the study winters between October and April. The model outputs analyzed included snow–soil interface temperature and energy fluxes at the snow surface.

Calculation

Even though the LAI values of the sites are observed using an optical method (Licor LAI-2000 Plant Canopy Analyzer), the commonly used correction factors may increase the value of LAI significantly. It is also possible to estimate LAI from hemispheric photos, using biomass based estimates or with remote sensing techniques. Further, SVF can be either determined optically (using Licor LAI-2000 Plant Canopy Analyzer) or by empirical relationships between LAI and SVF. There is no agreement yet among snow modelers on which method yields the best estimates of commonly used canopy parameters. It has been shown that the model output is sensitive to the canopy parameters (Rasmus *et al.* 2013), and furthermore, it is not known which parameter combination will reproduce the below-canopy radiation conditions most reliably.

In this study, we used six possible combinations for LAI and SVF (Table 1). In the 'optical effective' parameterization the values obtained by using the LAI-2000 were used for LAI and SVF without correction. In the 'optical corrected' parameterization the LAI values were corrected for needle clumping by a correction factor of 1.65 (Stenberg 1996). Two experimental functions, the 'Pomeroy SVF' and 'Canadian land surface scheme (CLASS) SVF' parameterizations, were also used to estimate the SVF from either effective or corrected optical LAI values, respectively (Verseghy *et al.* 1993; Pomeroy *et al.* 2002).

LAI shows a strong dependence on the canopy density, which is a measure of canopy closure. Empirical relationships can be applied to estimate the stand scale SVF as a function of stand scale LAI. Verseghy *et al.* (1993) proposed the following dependency:

$$\mathrm{SVF} = e^{-0.5 i_{\mathrm{LAI}}} \tag{1}$$

Table 1 | LAI and canopy openness (SVF) parameterizations used in the SNOWPACK simulations

	Pine, sparse		Pine, dense		Spruce	
Parameterization	**LAI**	**SVF**	**LAI**	**SVF**	**LAI**	**SVF**
Optical effective	1.58	0.33	1.93	0.19	2.62	0.29
Optical corrected	2.61	0.33	3.18	0.19	4.32	0.29
Optical effective, Pomeroy SVF	1.58	0.32	1.93	0.26	2.62	0.17
Optical effective, CLASS SVF	1.58	0.45	1.93	0.38	2.62	0.27
Optical corrected, Pomeroy SVF	2.61	0.17	3.18	0.11	4.32	0.03
Optical corrected, CLASS SVF	2.61	0.27	3.18	0.20	4.32	0.12

Optical effective is the direct observation with a Licor LAI-2000 Plant Canopy Analyzer. *Optical corrected* is a correction for needle clumping made by multiplying the apparent LAI value by 1.65 (Stenberg 1996). The *Pomeroy SVF* and *CLASS SVF* values for the SVF have been calculated by using the methods of Pomeroy *et al.* (2002) and Verseghy *et al.* (1993), respectively.

where i_{LAI} is the leaf area index. This dependency is used to calculate the 'CLASS SVF' parameterization in the present study.

Equation (1) is used, for example, in the CLASS for global circulation models, and it was originally developed for estimating long wave radiation in coniferous forests (Verseghy *et al.* 1993). The land surface scheme of the Swedish Rossby Centre regional climate model uses Equation (1) for all types of forest and for the estimation of both shortwave and longwave radiation (Samuelsson *et al.* 2006).

Pomeroy *et al.* (2002) suggested a method where canopy density and effective optical LAI are related by the function:

$$\begin{cases} C_c = 0 & i_{\mathrm{LAI}'} \le e^{-0.55/0.29} \\ C_c = 0.29 \ln (i_{\mathrm{LAI}'}) + 0.55 & e^{-0.55/0.29} \le i_{\mathrm{LAI}'} \le e^{0.45/0.29} \\ C_c = 1 & i_{\mathrm{LAI}'} > e^{0.45/0.29} \end{cases} \tag{2}$$

where $C_c$is the canopy density and $i_{\mathrm{LAI}'}$ is the winter effective LAI. These expressions assume that the canopy density is zero below a threshold value of 0.15 for LAI, and one above a threshold value of 4.72. The SVF can be obtained as:

$$\mathrm{SVF} = 1 - C_c \tag{3}$$

This function is used in the present study to obtain the 'Pomeroy SVF' parameterization.

RESULTS

Observed radiation components and temperature regimes

Mean air and snow–soil interface temperatures were nearly similar in the open field and in the pine forest during the early winter 2007–2008, but during mid-winter and melt period the open area had slightly higher air and snow–soil interface temperatures and the differences increased through the spring (Figure 2(a)). Air temperatures did not differ among the forest sites. At the pine site, snow–soil interface temperatures were higher below the sparse pine canopy during the snow season of winter 2008–2009, but the ground was warmer below the dense canopy after snow melt (Figure 2(b)). During the winter 2009–2010, the snow–soil interface temperatures in the pine forest were consistently higher than the ones in the spruce forest (Figure 2(c)).

Not surprisingly, the open field received clearly larger amounts of shortwave radiation compared to the pine forest floor (Figure 3(a)), and incoming shortwave radiation values were all the time higher below the pine canopy compared to the spruce forest (Figure 3(c)). At the pine forest site, the location with a sparse canopy received higher amounts of incoming shortwave radiation compared with the location with a dense canopy (Figure 3(b)). During the mid-winter, differences were small. The difference between the hourly values was largest during spring and at mid-day (data not shown).

Longwave radiation levels were lower at the open field compared to the site with the sparse pine canopy (Figure 4(a)). Differences among the forest sites were small, but during the early and late winter the dense pine canopy location received more incoming longwave radiation than the sparse canopy location at the pine site (Figure 4(b)) and the spruce forest site received more incoming longwave radiation than the pine forest site (Figure 4(c)). No daily cycle could be seen in the differences among the site in longwave radiation (data not shown).

The absolute differences among the sites increased toward the spring, especially in the monthly mean incoming shortwave but also in the longwave radiation (Table 2). The pattern is less clear in the relative differences. Maximum differences between the study environments are seen during the afternoon hours, both in absolute and relative terms (Table 3).

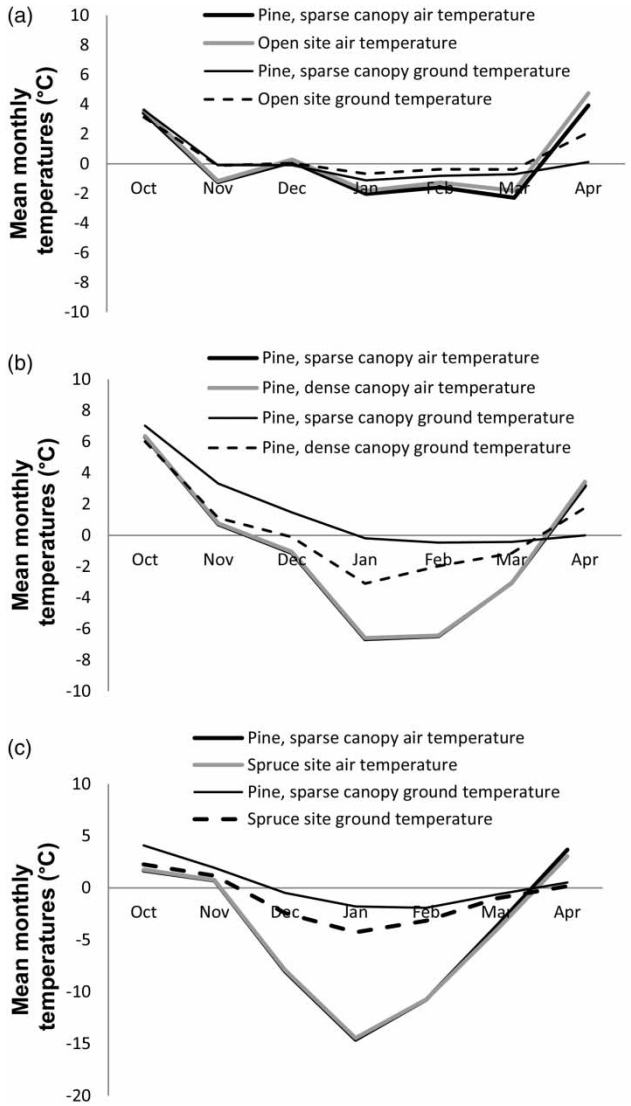

Figure 2 | Observed mean monthly air and snow–soil interface temperatures in the open field and (a) below the sparse pine canopy during the winter 2007–2008, (b) below the sparse and the dense pine canopy during the winter 2008–2009 and (c) below the sparse pine and the spruce canopy during the winter 2009–2010.

Comparisons between snow model SNOWPACK simulations and observations

Snow depth simulations had a reasonably good quality during the winters (Figure 5). Effect of canopy parameterization is

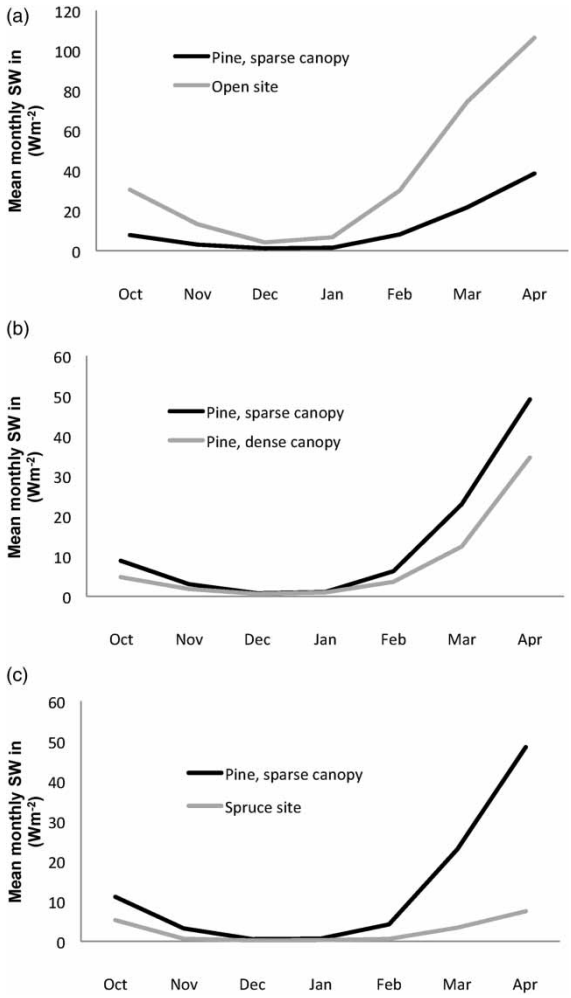

Figure 3 | Observed mean monthly incoming shortwave radiation in the open field and (a) below the sparse pine canopy during the winter 2007–2008, (b) below the sparse and the dense pine canopy during the winter 2008–2009 and (c) below the sparse pine and the spruce canopy during the winter 2009–2010.

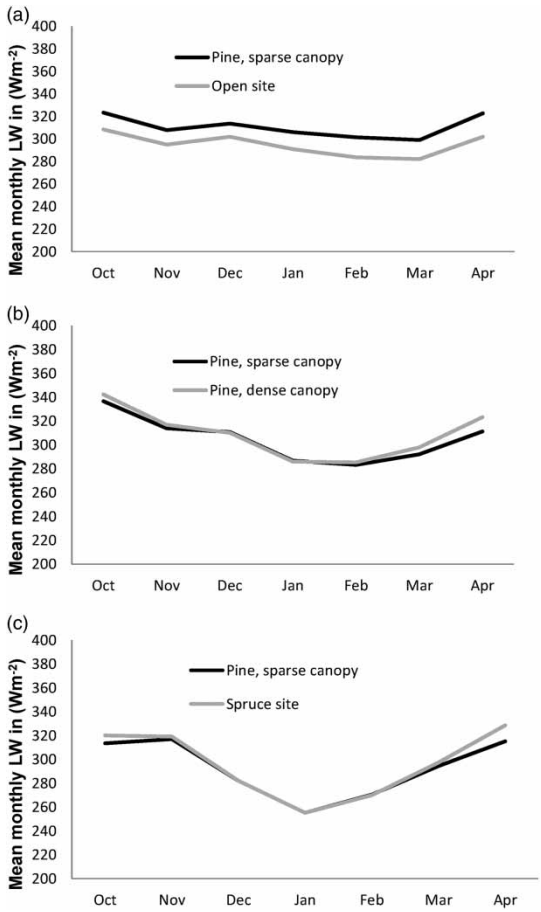

Figure 4 | Observed mean monthly incoming longwave radiation in the open field and (a) below the sparse pine canopy during the winter 2007–2008, (b) below the sparse and the dense pine canopy during the winter 2008–2009 and (c) below the sparse pine and the spruce canopy during the winter 2009–2010.

very clear in snow amount simulations. When LAI and SVF are larger, also their range, caused by the different estimation methods, grows. This is seen when comparing the simulations below the pine and spruce canopies, especially during winter 2009/2010, when the snow depth was approximately twice that during the previous winter. The role of snow interception grows during a snow-rich winter, and the same applies to canopy parameterization governing the interception calculations.

Overall, the choice of canopy parameters had only a small effect on the snow–soil interface temperature in the model simulations (Figure 6 and Table 4). Because of large range in the spruce canopy LAI estimates, range of simulated interception is also large – this has an indirect effect on the simulated snow–soil interface temperature below the spruce canopy through affecting the snow depth simulations (Figure 6(d)). Typically, the simulated snow–soil interface temperatures were too low compared with the measured temperatures during the snow season below the forest canopies. A good correspondence between the simulated and observed temperatures was found only at the dense canopy location at the pine site in the winter 2008–2009 (Figure 6(b)).

The canopy parameterizations including a LAI estimate with a needle clumping correction factor produced simulated shortwave radiation amounts that were closer to those measured at both the pine and the spruce sites (Figure 7 and Table 4). On the other hand, the parameterizations using corrected LAI and either of the empirical

Table 2 | Mean monthly differences (absolute, Wm^{-2}, and in percent, sparse pine site values used as reference values) observed in (a) incoming shortwave and (b) longwave radiation among the study environments

	Sparse pine–Open (winter 2007/2008)		Sparse–Dense pine (winter 2008/2009)		Sparse pine–Spruce (winter 2009/2010)	
	Abs	%	Abs	%	Abs	%
(a)						
October	−19	−91	5	19	6	21
November	−10	−133	1	15	2	32
December	−3	−62	0	7	0	20
January	−5	−116	0	−2	0	18
February	−22	−123	3	15	4	21
March	−25	−127	8	18	18	41
April	−72	−108	21	20	42	45
(b)						
October	16	5	−6	−2	−7	−2
November	13	4	−3	−1	−2	−1
December	12	4	1	0	0	0
January	15	5	1	0	0	0
February	18	6	−2	−1	1	0
March	16	5	−6	−2	−3	−1
April	19	6	−12	−4	−13	−4

Table 3 | Mean differences (absolute, Wm^{-2}, and in percent, sparse pine site values used as reference values) observed during different hours of the day in incoming (a) shortwave and (b) longwave radiation among the study environments

	Sparse pine–Open (winter 2007/2008)		Sparse–Dense pine (winter 2008/2009)		Sparse pine–Spruce (winter 2009/2010)	
	Abs	%	Abs	%	Abs	%
(a)						
0–6	0	10	−0	0	−0	−1
6–12	−25	−170	5	17	11	37
12–18	−60	−301	17	29	29	68
18–24	−1	−10	1	6	1	9
(b)						
0–6	13	4	−3	−1	−3	−1
6–12	13	5	−3	−1	−3	−1
12–18	18	6	−5	−2	−3	−1
18–24	17	6	−4	−1	−4	−1

relationships between LAI and SVF produced lower incoming shortwave radiation values for the spruce canopy than those measured (Figure 7(d)). The parameterization using the optical estimate of both LAI and SVF seemed to give slightly higher values in these conditions also.

In all cases, the simulated longwave radiation fluxes were underestimated compared to measured values (Figure 8 and Table 4). The simulated fluxes best fit those measured below the spruce canopy. Across all forest types the canopy parameterizations using the corrected LAI gave the best correspondence between the simulation results and the observations.

Comparison of the absolute differences between the simulated and observed mean monthly snow–soil interface temperature and incoming radiation fluxes also indicated that the use of the corrected LAI values better approximates the observations than the use of the uncorrected effective LAI (data not shown). SVF could be either optically estimated or based on empirical equation. In most of the cases the error in incoming shortwave radiation increased toward the spring. If simulated values were higher than the observed ones during the winter months, the situation may be reversed during April. These seasonal patterns indicate a model deficiency related to solar elevation angle. The solar elevation angle was taken into account in the model, both in the direct beam absorption coefficient and in the modification of the direct beam SVF. In both cases, the model parameterization should increase the shortwave transmission as a function of increasing solar angle. It should also be noted that most of the seasonal deviation in downward shortwave radiation was reduced by using the optical corrected LAI and the higher SVF estimates in the model. The impact of local gaps in the forest canopies and the corresponding sensitivity to solar elevation angle and time of the year could however be further taken into account, either by calibration of the canopy transmissivity parameters or by detailed canopy gap fraction modeling using hemispherical photos following Musselman *et al.* (2012a, b). The impact of local gaps was also pointed out by Stähli *et al.* (2009) using below-canopy radiation measurements along a 10 m rail. Error in incoming longwave radiation was more constant over time, with a systematic underestimation of about 10–20 Wm^{-2} independent of forest stand but with a clearly better results for simulations with the optical corrected LAI and as small SVF as possible. Snow–soil interface temperature was highly sensitive to the choice of

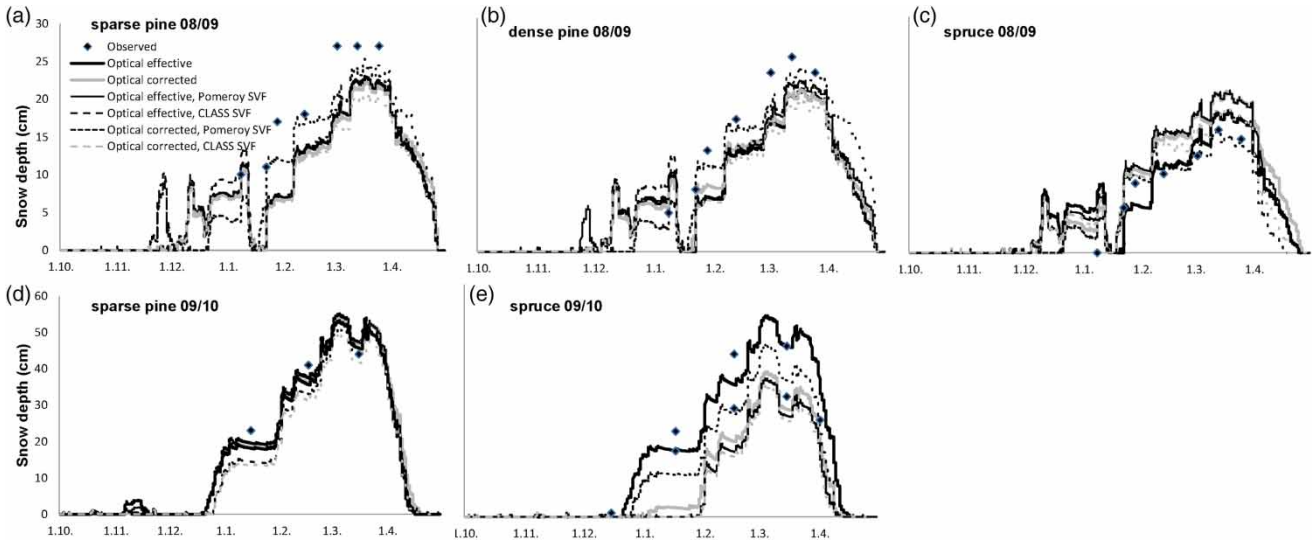

Figure 5 | Simulated snow depths using the LAI and canopy openness (SVF) parameterizations listed in Table 1: winter 2008–2009, (a) sparse pine; (b) dense pine and (c) spruce canopy; winter 2009–2010, (d) sparse pine and (e) spruce canopy. Dots mark the observations from the site.

parameterization only in the spruce forest case; quality of these simulations was linked to the quality of snow depth simulations (Figure 5). A general decrease was seen in the differences toward the spring. When comparing the sparse pine forest cases during winters 2008–2009 and 2009–2010, differences between the simulations and observations were generally larger during the winter 2009–2010 with thicker snow cover.

Effect of input data on simulation quality

The effect of input data time resolution as well as the choice of different type of above canopy radiation input could be considered using the open field and pine forest below-canopy observations during winter 2007/2008 – the observation station provided data with higher temporal resolution than FMI observations. Simulations using either 3 h or 30 min resolution showed only minor differences in radiation component outputs (data not shown). Experimenting with different possible above canopy shortwave radiation inputs (observations from the open field, observations from a site Jokioinen with a distance of 100 km to Evo, FMI grid estimates) showed some variability in simulated radiation levels below the canopy, as expected. Still, the variation caused by different canopy parameterizations (Figure 9(a), gray lines) was larger than the variation caused by above canopy radiation from different sources (black lines). The situation was more complicated in the longwave radiation simulations, where the effect of the source of the longwave data (Figure 9(b), black lines) was approximately of the same order of magnitude as the effect of canopy parameterization (gray lines). The use of observed open field radiation improved the below-canopy longwave radiation simulations compared to the use of the FMI grid estimate of the shortwave radiation, and longwave radiation derived from it.

DISCUSSION AND CONCLUSIONS

The observations on near surface radiation and temperature conditions in southern boreal forests with different canopy conditions reinforce previous findings on the importance of canopy and canopy distribution on winter time snow surface mass and energy balance (Hedström & Pomeroy 1998; Lundberg & Koivusalo 2003; Stähli *et al.* 2009).

The effects of tree species were clearly seen in the observations. Incoming shortwave radiation values were higher in the pine forest compared to the spruce forest at all times, and because of the dense canopy structure, the spruce forest had higher incoming longwave radiation levels below the canopy than the pine forest. Differences in

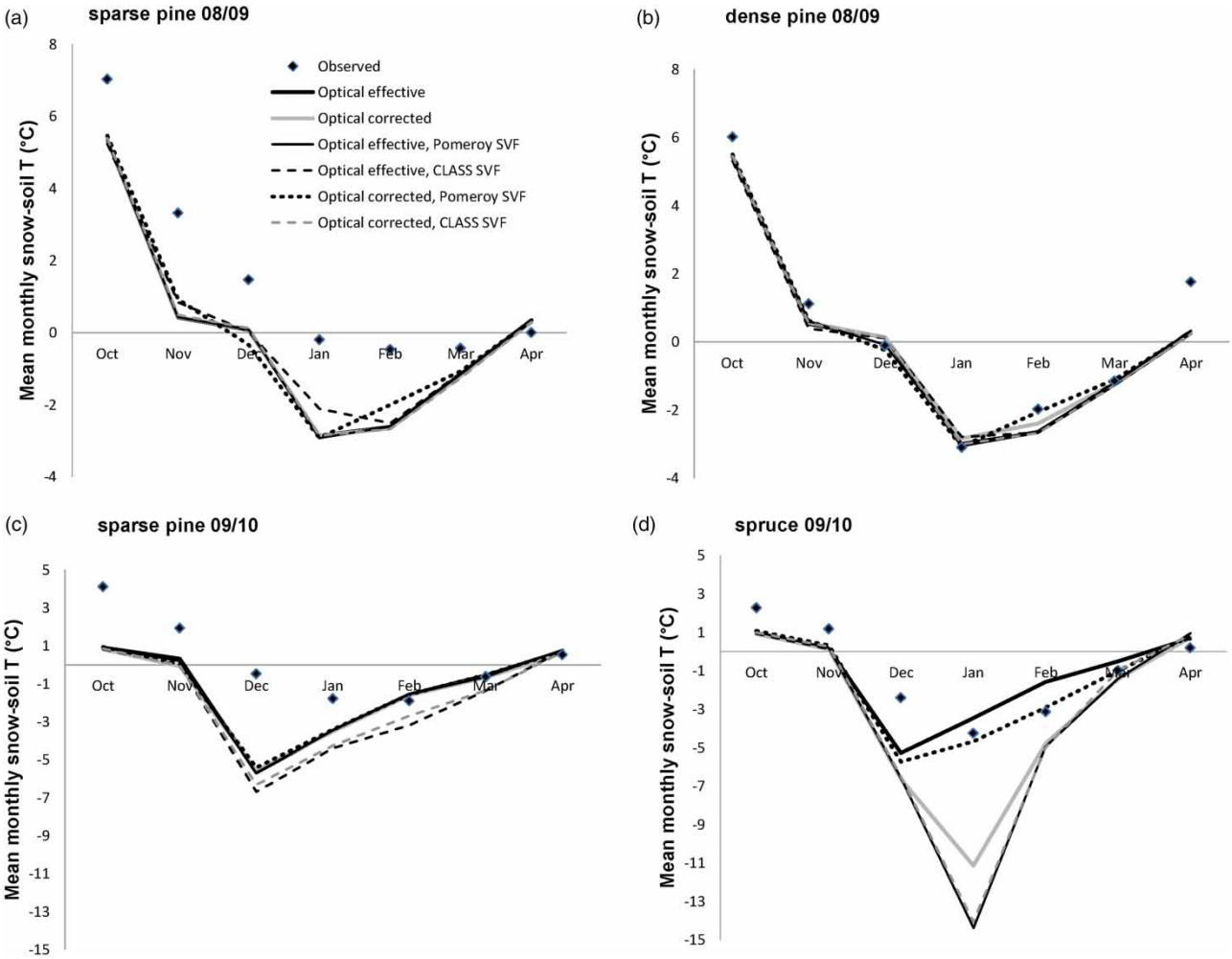

Figure 6 | Simulated mean monthly snow–soil interface temperatures using the LAI and canopy openness (SVF) parameterizations listed in Table 1 during winter 2008–2009 in the pine forest with (a) sparse canopy and (b) dense canopy and during winter 2009–1010 in the (c) sparse pine forest and in the (d) spruce forest. Dots mark the observations from the site.

incoming longwave radiation levels between the pine and spruce sites are caused by notable differences in LAI and SVF between the sites, but they may also may be due partly to structural differences, such as branch orientation, in the canopies of different tree species. The forest snow–soil interface temperatures were higher below the sparse pine canopy during the snow season, but the ground warmed more efficiently below the dense canopy after snow melt. This can be explained by the slightly thicker snow cover (and slightly delayed snow melt) below the sparse canopy. Higher levels of incoming shortwave radiation were observed below the sparse pine canopy, and a slight tendency toward lower incoming longwave radiation flux was also seen.

Differences in observed radiation flux values, both absolute and relative, were highest during the afternoon hours of the day and increased toward the spring. This suggests that a relatively small error in the canopy cover estimate for a hydrological or climate model may lead to large uncertainties in the surface flux estimates during those times.

Canopy parameter values had a great effect on the quality of sub-canopy snow mass and energy balance simulations by the SNOWPACK model. The model output is especially sensitive to the canopy density and the tree species (characterized in the model by LAI and SVF); aspects like leaf orientation or canopy structure, varying between the species, are not taken into account. In most of the cases, the simulation results of radiative terms, snow depth or

Table 4 | Root-mean-squared errors between the SNOWPACK simulation outputs obtained using the parameterizations in Table 1 and the observations

	Optical effective	Optical corrected	Optical effective, Pomeroy SVF	Optical effective, CLASS SVF	Optical corrected, Pomeroy SVF	Optical corrected, CLASS SVF
Snow–soil interface temperature						
Sparse pine 2008–2009	2.54	2.48	2.57	2.33	2.41	2.48
Dense pine 2008–2009	1.72	1.69	1.74	1.84	1.66	1.71
Sparse pine 2009–2010	3.30	3.33	3.34	3.80	3.21	3.58
Spruce 2009–2010	2.14	3.85	4.89	2.14	2.07	4.78
Incoming shortwave radiation						
Sparse pine 2008–2009	24.95	18.22	24.84	27.99	19.49	18.35
Dense pine 2008–2009	22.61	17.02	24.53	28.04	17.71	16.98
Sparse pine 2009–2010	27.22	21.17	27.13	29.84	22.35	21.30
Spruce 2009–2010	10.72	5.72	6.77	10.72	6.34	5.62
Incoming longwave radiation						
Sparse pine 2008–2009	24.33	19.67	24.19	28.01	15.24	17.96
Dense pine 2008–2009	20.48	15.14	23.03	27.20	12.50	15.68
Sparse pine 2009–2010	29.01	24.21	28.86	32.75	19.42	22.37
Spruce 2009–2010	16.93	15.03	13.90	16.93	11.60	12.05

snow–soil interface temperature had the best agreement with the measurements when using a combination of optically obtained LAI values with needle clumping correction (Stenberg 1996) and either optical or empirical SVF values as a canopy parameterization.

The discrepancies seen in some of the snow–soil interface temperature simulations are most probably linked with the occasional difficulties to correctly simulate the snow accumulation and canopy interception. Owing to unstable weather during autumn, it is normal at the study sites for the snow cover to form and melt several times, before settling rather late during the early winter. Problems in the snow cover formation timing can cause discrepancies between simulated and observed snow–soil interface temperatures. Comparison with snow accumulation data from a nearby FMI station showed that the model captured quite well the snowless and snow covered periods during the early winter, although the snow depths may not be precise. There could be couple of days mismatch in the final formation date. Canopy and canopy parameterization affected the melt rate and melt date of the simulated snow cover, but although the canopy estimates had effects on snow accumulation, formation date of the simulated snow cover was not highly sensitive to the canopy. The bottom boundary conditions of the SNOWPACK model, including the rough parameterization of the soil column properties, especially of heat conductivity, and perhaps an unrealistic initial temperature profile may also have affected the simulation results. There is also naturally uncertainty in manual snow depth observations.

Pomeroy *et al.* (2009) showed that the level of downwelling longwave radiation below the canopy, observed in their study, was enhanced because the canopy, warmed by absorbed shortwave radiation, re-radiated the energy absorbed as longwave radiation. Thus, using air temperature as an approximation of the canopy temperature leads to an underestimation of the energy balance term related to longwave radiation below coniferous canopies. In a previous study using the SNOWPACK model, which simulates the canopy temperature, a problem with the longwave transmissivity simulations was shown to be associated with too high canopy temperatures and overestimation of the longwave radiation (Stähli *et al.* 2009). In contrast to the latter study, the results presented here showed an underestimation of longwave radiation which was rather constant in time, around 10–20 Wm^{-2} on a monthly basis, without any clear seasonal dependence. The use of corrected LAI values (higher values compared to the effective LAI) and the smallest SVF values reduces the relative importance of

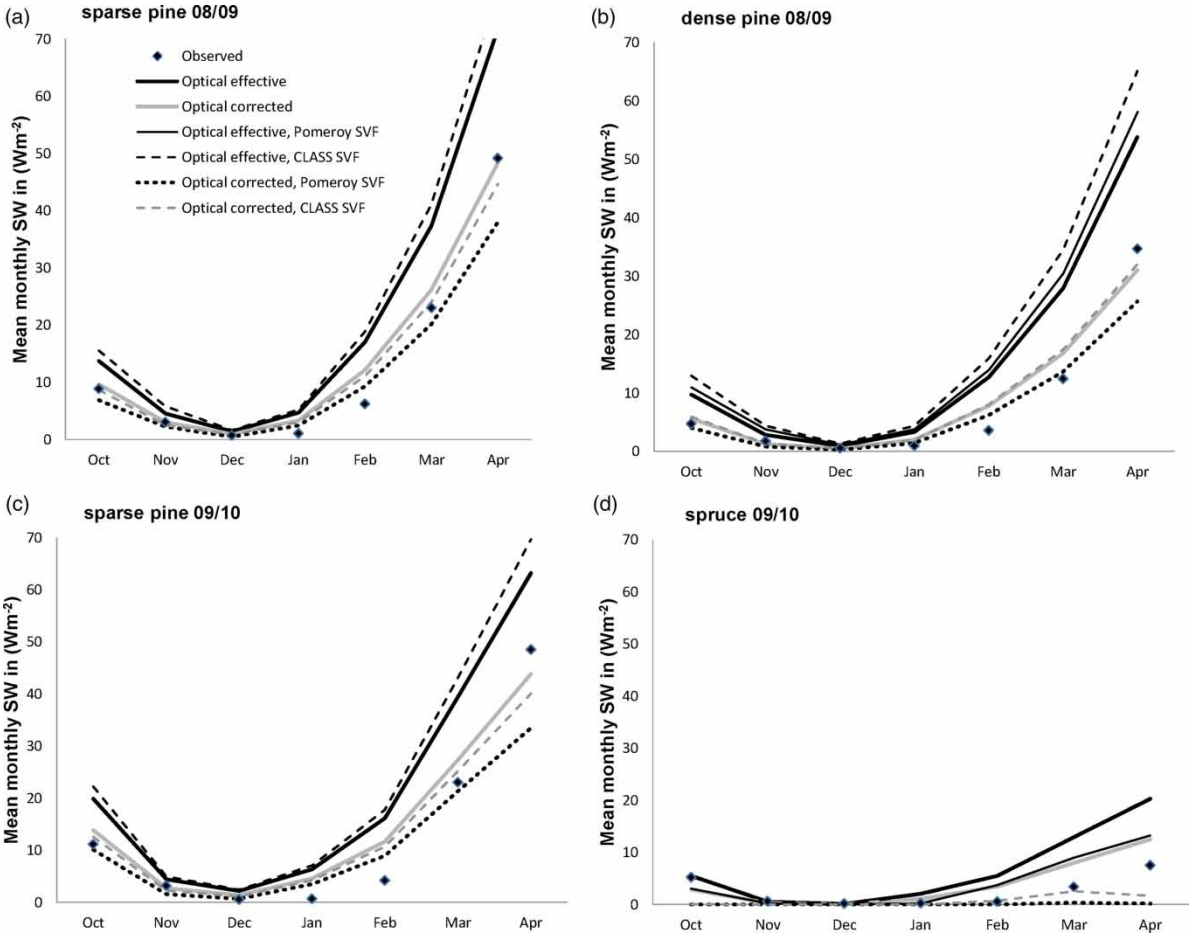

Figure 7 | Simulated mean monthly incoming shortwave radiation using the LAI and canopy openness (SVF) parameterizations listed in Table 1 during winter 2008–2009 in the pine forest with (a) sparse canopy and (b) dense canopy and during winter 2009–1010 in the (c) sparse pine forest and in the (d) spruce forest. Dots mark the observations from the site.

the atmospheric longwave radiation and increases the importance of the longwave radiation emitted by the canopy. The simulated longwave radiation below the canopy was systematically improved using this parameterization, without increasing seasonal deviations. This suggests that the underestimation of below-canopy longwave radiation could also be a function of errors in the estimation of atmospheric longwave radiation, and not only related to seasonal or diurnal dynamics in the canopy longwave radiation emission.

For snow–soil interface temperatures, the differences in model performance were rather small compared to the magnitude of the underestimation during the cold winter months. There was a tendency that the simulations with higher SVF had a larger underestimation of snow–soil interface temperatures as well as slightly larger underestimation of longwave radiation, suggesting that the longwave radiation balance is governed more by the SVF than by the LAI, and that the best SVF estimate with regard to this particular longwave model was given by the Pomeroy function, followed second by the optical estimates and thirdly by the CLASS model. However, for shortwave radiation, the optical measured SVF gave the best results followed by the CLASS function and the Pomeroy function last. The snow depth simulations were more influenced by the SVF parameterizations in years with less snow, and more by the LAI estimates in years with more snow. This is logical since the direct throughfall and interception capacity are directly linked to SVF and LAI, respectively, in the model. In snow-rich years, simulated snow depths were closer to observations when using the optical effective LAI, which is in line with Hedstrom & Pomeroy (1998) who suggested that effective LAI should be more related to snow

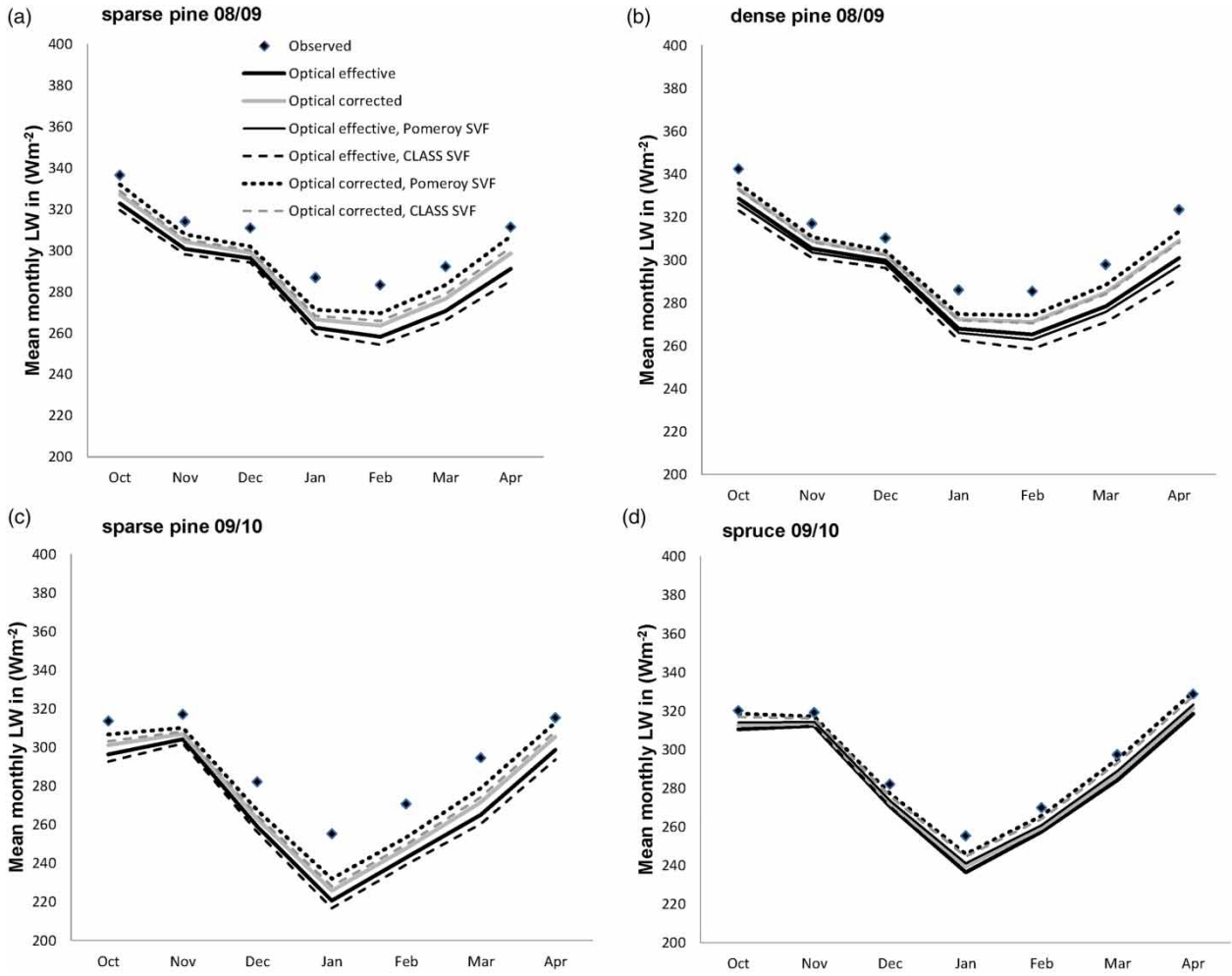

Figure 8 | Simulated mean monthly incoming longwave radiation using the LAI and canopy openness (SVF) parameterizations listed in Table 1 during winter 2008–2009 in the pine forest with (a) sparse canopy and (b) dense canopy, and during winter 2009–1010 in the (c) sparse pine forest and in the (d) spruce forest. Dots mark the observations from the site.

interception capacity, whereas the double-sided LAI would be more relevant for liquid water interception. In years and sites where SVF were more important for the similarity between observed and simulated snow depth, the best simulations were obtained with the higher SVF values, suggesting that direct throughfall is exceeding the SVF estimated by optical measurements. In summary, these results suggest that LAI corrected for clumping is the most appropriate for radiation transmission modeling, whereas effective LAI is most appropriate for snow interception modeling. It is also clear that the seasonal behavior of canopy shortwave radiation transmission, most likely linked to solar elevation and impact of local gaps in the canopy, need to be better described to improve modeling of local conditions, such as those represented by the observations in this study.

The seasonal differences in simulation and observation of shortwave radiation transmission were to a large degree reduced by using the LAI corrected for needle clumping and the higher estimates of SVF. The diurnal differences in simulated and observed shortwave radiation were more likely an effect of unsymmetrical distribution of local gaps in the forest canopies, perhaps related to adaption of the trees to the dominating direction of shortwave radiation coming from the south at low solar angles at these high latitude Finnish sites, or changes in the branch orientation due to stem moisture conditions. The differences in diurnal longwave radiation between simulations and observations could instead be related to the lack of canopy heat storage in the model, since a canopy heat storage would decrease and delay the diurnal canopy temperature cycle, and the

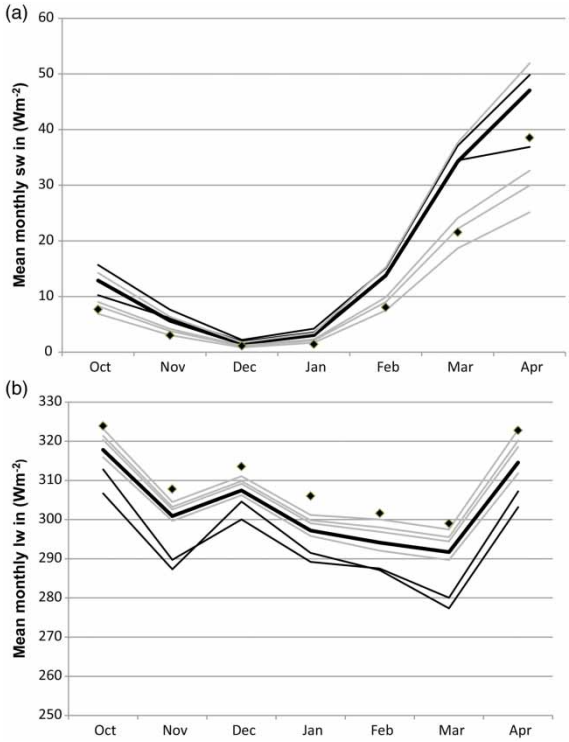

Figure 9 | Effect of canopy parameterizations vs. source of the above canopy radiation input for (a) shortwave and (b) longwave radiation during winter 2007–2008 in the pine forest with sparse canopy. Dots mark the observations; black lines represent the simulations with different radiation input but the same canopy parameterization (optical effective); gray lines the simulations with different canopy parameterization but the same radiation input (observations from the open field). Thick black shows the simulation with optical effective parameterization and the observed radiation input.

corresponding emission of longwave radiation from the canopy. The model version used in the current paper did not include canopy heat storage, and this hypothesis could not be tested. However, in a recent study by Gouttevin *et al.* (2015), canopy heat storage was introduced in the SNOWPACK canopy model, which improved both canopy trunk temperatures and below-canopy longwave radiation.

Effect of time resolution was very small in our results. Also the use of FMI grid estimates of the incoming shortwave radiation did not seem to play a significant role in interpretation of the simulation outputs below the canopy. The situation was different with the longwave radiation. The use of observed radiation from the nearby open field significantly improved the below-canopy longwave radiation simulations compared to the use of the FMI grid estimate of the shortwave radiation, and longwave radiation derived from it. All of the simulation outputs underestimated the observed below-canopy radiation levels; the underestimation was less in the simulations that used the observed radiation as input.

The effect of the forest canopy is, at its best, described in simple ways in snow, hydrological and climate models (e.g. Essery 1998; Rutter *et al.* 2009). Variation between different forest types is seldom taken into account, and consideration of variation inside a forest is normally omitted. Additional variations among the results of simulations are introduced by the different possible values for the commonly used canopy parameters LAI and canopy openness (SVF). It is also clear that the study was limited (a single set of instruments within each canopy). Nevertheless, detailed mapping of the site, including mapping of LAI and SVF (presented in Rasmus *et al.* (2011)) facilitated finding representative locations for the instruments, and even though the results cannot acknowledge the small-scale variability of the energy balance terms, the study gives a realistic estimate of the range of the radiation levels experienced in these southern boreal forests. One way forward is an ensemble-type approach, where a set of LAI and SVF is given as model input, and a corresponding set of model outputs is produced, expressing the natural variability in radiation (and snow) conditions within the forest.

Spatial variability of the boreal forest canopy, leading to variability in seasonal snow cover through spatial differences in snow mass and energy balance, may have significant ecological consequences. Evergreen dwarf shrubs such as lingonberry have been shown to retain their photosynthetic capacity through the winter, although the photosynthesis below the snow is strongly light-limited (Lütz *et al.* 2005; Lundell *et al.* 2008, 2010; Saarinen & Lundell 2010). Depending on the snow and light conditions, subnivean photosynthesis has been estimated to compensate for a significant part of the daily respiratory losses of these plants even at the low PAR levels prevailing under the snow (Starr & Oberbauer 2003). Spatial variation in snow cover, leading to variation in temperature and PAR regimes, can thus affect species composition on a range of scales, and be a factor in shaping vegetation both at the landscape and at the stand level.

ACKNOWLEDGEMENTS

Hanna Leisti, Olli-Kalle Kauppinen and Tuomas Niskanen assisted us with the fieldwork. The Lammi biological station

and the HAMK University of Applied Sciences provided logistic support. Heikki Hänninen and Helena Åström from the PECC-group are acknowledged for their valuable support on this project. Our research was funded through the Academy of Finland (Project numbers 115532 and 122194), the Environmental Research Center of the University of Helsinki HERC, the Finnish Cultural Foundation, the Maj and Tor Nessling Foundation, the Jenny and Antti Wihuri Foundation and Svenska kulturfonden.

REFERENCES

Bartelt, P. & Lehning, M. 2002 A physical SNOWPACK model for the Swiss avalanche warning: Part I. Numerical model. *Cold Reg. Sci. Technol.* **35**, 123–145.

Bernier, P. Y. & Swanson, R. H. 1993 The influence of opening size on snow evaporation in the forests of the Alberta foothills. *Can. J. For. Res.* **23**, 239–244.

Billings, W. D. & Bliss, L. C. 1959 An alpine snowbank environment and its effects on vegetation, plant development, and productivity. *Ecology* **40**, 388–397.

Blyth, E. M., Harding, R. J. & Essery, R. L. H. 1999 A coupled dual source GCM SVAT. *Hydrol. Earth Syst. Sci.* **3**, 71–84.

Chen, J. M., Blanken, P. D., Black, T. A., Guilbeault, M. & Chen, S. 1997 Radiation regime and canopy architecture in a boreal aspen forest. *Agric. For. Meteorol.* **86**, 107–125.

Curl, H., Hardy, T. & Ellermeier, R. 1972 Spectral absorption of solar radiation in alpine snowfields. *Ecology* **53**, 1189–1194.

Davis, R. E., Hardy, J. P., Ni, W., Woodcock, C., McKenzie, J. C., Jordan, R. & Li, X. 1997 Variation of snow cover ablation in the boreal forest: a sensitivity study on the effects of conifer canopy. *J. Geophys. Res.* **102**, 29389–29296.

Essery, R. 1998 Boreal forests and snow in climate models. *Hydrol. Processes* **12**, 1561–1567.

Essery, R., Pomeroy, J., Ellis, C. & Link, T. 2008 Modelling longwave radiation to snow beneath forest canopies using hemispherical photography or linear regression. *Hydrol. Processes* **22**, 2788–2800.

Gerland, S., Winther, J. G., Ørbæk, J. B., Liston, G. E., Øritsland, N. A., Blanco, A. & Ivanov, B. 1999 Physical and optical properties of snow covering Arctic tundra on Svalbard. *Hydrol. Processes* **13**, 2331–2343.

Gouttevin, I., Lehning, M., Jonas, T., Gustafsson, D. & Mölder, M. 2015 A two-layer canopy with thermal inertia for an improved modelling of the sub-canopy snowpack energy-balance. *Geosci. Model Dev. Discuss.* **8**, 209–262, doi: 10.5194/gmdd-8–209–2015.

Gryning, S. E., Batchvarova, E. & DeBruin, H. A. R. 2001 Energy balance of a sparse coniferous high-latitude forest under winter conditions. *Boundary-Layer Meteorol.* **99**, 465–488.

Harding, R. J. & Pomeroy, J. W. 1996 The energy balance of the winter boreal landscape. *J. Clim.* **9**, 2778–2787.

Hardy, J. P., Melloh, R., Koenig, G., Marks, D., Winstral, A. & Pomeroy, J. W. 2004 Solar radiation transmission through conifer canopies. *Agric. For. Meteorol.* **126**, 257–270.

Hardy, J. P. & Albert, M. 1995 Snow-induced thermal variations around a single conifer tree. *Hydrol. Processes* **9**, 923–933.

Hedström, N. R. & Pomeroy, J. W. 1998 Measurements and modelling of snow interception in the boreal forest. *Hydrol. Processes* **12**, 1611–1625.

Koivusalo, H. & Kokkonen, T. 2002 Snow processes in a forest clearing and in a coniferous forest. *J. Hydrol.* **262**, 145–164.

Konzelmann, T., van de Wal, R. S. W., Greuell, W., Bintanja, R., Henneken, E. A. C. & Abe-Ouchi, A. 1994 Parameterization of global and longwave incoming radiation for the Greenland Ice Sheet. *Glob. Planet. Chang.* **9**, 143–164.

Lehning, M., Bartelt, P., Brown, B., Russi, T., Stöckli, U. & Zimmerli, M. 1998 SNOWPACK Model calculations for avalanche warning based upon a network of weather and snow stations. *Cold Reg. Sci. Technol.* **30**, 145–157.

Lehning, M., Bartelt, P., Brown, B., Fierz, C. & Satyawali, P. 2002a A physical SNOWPACK model for the Swiss avalanche warning. Part II. Snow microstructure. *Cold Reg. Sci. Technol.* **35**, 147–167.

Lehning, M., Bartelt, P., Brown, B. & Fierz, C. 2002b A physical SNOWPACK model for the Swiss avalanche warning service. Part III. Meteorological forcing, thin layer formation and evaluation. *Cold Reg. Sci. Technol.* **35**, 169–184.

Lehning, M., Völksch, I., Gustafsson, D., Nguyen, T., Stähli, M. & Zappa, M. 2006 ALPINE3D: a detailed model of mountain surface processes and its application to snow hydrology. *Hydrol. Processes* **20**, 2111–2128.

Link, T. E. & Marks, D. 1999 Distributed simulation of snowcover mass- and energy-balance in the boreal forest. *Hydrol. Processes* **13**, 2439–2452.

Lundberg, A. & Koivusalo, H. 2003 Estimating winter evaporation in boreal forests with operational snow course data. *Hydrol. Processes* **17**, 1479–1493.

Lundell, R., Saarinen, T., Åström, H. & Hänninen, H. 2008 The boreal dwarf shrub Vaccinium vitis-idaea retains its capacity for photosynthesis through the winter. *Botany* **86**, 491–500.

Lundell, R., Saarinen, T. & Hänninen, H. 2010 Effects of snowmelt on the springtime photosynthesis of the evergreen dwarf shrub *Vaccinium vitis-idaea*. *Plant Ecol. Div.* **2**, 121–130.

Lundy, C., Brown, R. L., Adams, E. E., Birkeland, K. W. & Lehning, M. 2001 A statistical validation of the SNOWPACK model in a Montana climate. *Cold Reg. Sci. Technol.* **33**, 237–246.

Lütz, C., Shönauer, E. & Neuner, G. 2005 Physiological adaptation before and after snow melt in green overwintering leaves of some alpine plants. *Phyton* **45**, 139–156.

Marks, D. & Dozier, J. 1992 Climate and energy exchange at the snow surface in the alpine region of the Sierra Nevada, 2,

snow cover energy balance. *Water Resour. Res.* **28**, 3043–3043.

Marks, D., Reba, M., Pomeroy, J., Link, T., Winstral, A., Flerchinger, G. & Elder, K. 2008 Comparing simulated and measured sensible and latent heat fluxes over snow under a pine canopy to improve an energy balance snowmelt model. *J. Hydrometeorol.* **9**, 1506–1522.

Melloh, R. A., Hardy, J. P., Davis, R. E. & Robinson, P. B. 2001 Spectral albedo/reflectance of littered forest snow during the melt season. *Hydrol. Processes* **15**, 3409–3422.

Musselman, K. N., Molotch, N. P., Margulis, S. A., Kircher, P. B. & Bales, R. C. 2012a Influence of canopy structure and direct beam solar irradiance on snowmelt rates in a mixed conifer forest. *Agric. For. Meteorol.* **161**, 46–56.

Musselman, K. N., Molotch, N. P., Margulis, S. A., Lehning, M. & Gustafsson, D. 2012b Improved snowmelt simulations with a canopy model forced with photo-derived direct beam canopy transmissivity. *Water Resour. Res.* **48**, W10509, doi: 10.1029/2012WR012285.

Musselman, K. N., Margulis, S. A. & Molotch, N. P. 2013 Estimation of solar direct beam transmittance of conifer canopies from airborne LiDAR. *Rem. Sens. of Environ.* **136**, 402–415.

Økland, R. H., Rydgren, K. & Økland, T. 1999 Single-tree influence on understorey vegetation in a Norvegian Boreal spruce Forest. *Oikos* **87**, 488–498.

Pomeroy, J. W. & Dion, K. 1996 Winter radiation extinction and reflection in a boreal pine canopy: measurements and modelling. *Hydrol. Processes* **10**, 1591–1608.

Pomeroy, J. W., Parviainen, J., Hedstrom, N. & Gray, D. M. 1998 Coupled modelling of forest snow interception and sublimation. *Hydrol. Processes* **12**, 2317–2337.

Pomeroy, J. W., Hanson, S. & Faria, D. 2001 Small-Scale variation in snowmelt energy in a boreal forest: An additional factor controlling depletion of snow cover. In: *Proceedings of the 58th Eastern Snow Conference*, pp. 85–96.

Pomeroy, J. W., Gray, D. M., Hedström, N. R. & Janowich, J. R. 2002 Physically Based Estimation of Seasonal Snow Accumulation in the Boreal Forest. In: *Proceedings of the 59th Eastern Snow Conference*, pp. 93–108.

Pomeroy, J. P., Rowlands, A., Hardy, J. P., Link, T. E., Marks, D., Essery, R., Sicart, J. E. & Ellis, C. 2008 Spatial variability of shortwave irradiance for snowmelt in forests. *J. Hydrometeorol.* **6**, 1482–1490.

Pomeroy, J. W., Marks, D., Link, T., Ellis, C., Hardy, J. & Rowlands, A. 2009 The impact of coniferous forest temperature on incoming longwave radiation to melting snow. *Hydrol. Processes* **23**, 2513–2525.

Rasmus, S., Grönholm, T., Lehning, M., Rasmus, K. & Kulmala, M. 2007 Validation of the SNOWPACK-model in five different snow zones in Finland. *Boreal Environ. Res.* **12**, 467–488.

Rasmus, S., Lundell, R. & Saarinen, T. 2011 Interactions between snow, canopy and vegetation in a boreal coniferous forest. *Plant Ecol. Divers.* **4**, 55–65.

Rasmus, S., Gustafsson, D., Koivusalo, H., Laurén, A., Grelle, A., Kauppinen, O.-K., Lagnvall, O., Lindroth, A., Rasmus, K., Svensson, M. & Weslien, P. 2013 Estimation of winter leaf area index and sky view fraction for snow modelling in boreal coniferous forests: consequences on snow mass and energy balance. *Hydrological Processes* **27**, 2876–2891.

Rautiainen, M., Stenberg, P. & Nilson, T. 2005 Estimating canopy cover in Scots pine stands. *Silva Fennica* **39**, 137–142.

Rowlands, A., Pomeroy, J., Hardy, J., Marks, D., Elder, K. & Melloh, R. 2002 Small-scale spatial variability of radiant energy for snowmelt in a mid-latitude sub-alpine forest. In: *Proceedings of the 59th Eastern Snow Conference*, pp. 109–118.

Rutter, N. & 50 others. 2009 Evaluation of forest snow processes models (SnowMIP2). *J. Geophys. Res.* **114**, D06111, doi: 10.1029/2008JD011063.

Saarinen, T. & Lundell, R. 2010 Overwintering of *Vaccinium vitis-idaea* in two subarctic microhabitats – a reciprocal transplantation experiment. *Polar Res.* **29**, 38–45.

Samuelsson, P., Gollvik, S. & Ullerstig, A. 2006 The land-surface scheme of the Rossby Centre regional atmospheric climate model (RCA3). Meteorologi 122. Swedish Meteorological and Hydrological *Institute,* Norrköping, Sweden.

Stähli, M. & Gustafsson, D. 2006 Long-term investigations of the snow cover in a subalpine semi-forested catchment. *Hydrol. Processes* **20**, 411–428.

Stähli, M., Jonas, T. & Gustafsson, D. 2009 The role of snow interception in winter-time radiation processes of a coniferous sub-alpine forest. *Hydrol. Processes.* **23**, 2498–2512.

Starr, F. & Oberbauer, S. F. 2003 Photosynthesis of arctic evergreen shrubs under snow: implications for tundra ecosystem carbon balance. *Ecology* **84**, 1415–1420.

Stenberg, P. 1996 Correcting LAI-2000 estimates for the clumping of needles in shoots of conifers. *Agric. For. Meteorol.* **79**, 1–8.

Storck, P., Kern, T. & Bolton, S. 1999 Measurement of differences in snow accumulation, melt, and micrometeorology due to forest harvesting. *Northwest Sci.* **73**, 87–100.

Taconet, O., Bernard, R. & Vidal-Madjar, D. 1986 Evapotranspiration over an agricultural region using a surface flux/temperature model based on NOAA-AVHRR data. *Anglais* **25**, 284–307.

Veatch, W., Brooks, P. D., Gustafson, J. R. & Molotch, N. P. 2009 Quantifying the effects of forest canopy cover on net snow accumulation at a continental, mid-latitude site. *Ecohydrol.* **2**, 115–128.

Verseghy, D. L., McFarlane, N. A. & Lazare, M. 1993 CLASS–A Canadian land surface scheme for GCMs, II. Vegetation model and coupled runs. *Int. J. Climatol.* **13**, 347–370.

Vestergren, T. 1902 Om den olikformiga snöbetäckningens inflytande på vegetationen i Sarjekfjällen [On the influence of variations in snow cover on the vegetation in the Sarek mountains]. *Botaniska Notiser* **1902**, 241–268.

First received 25 September 2014; accepted in revised form 1 May 2015. Available online 23 June 2015